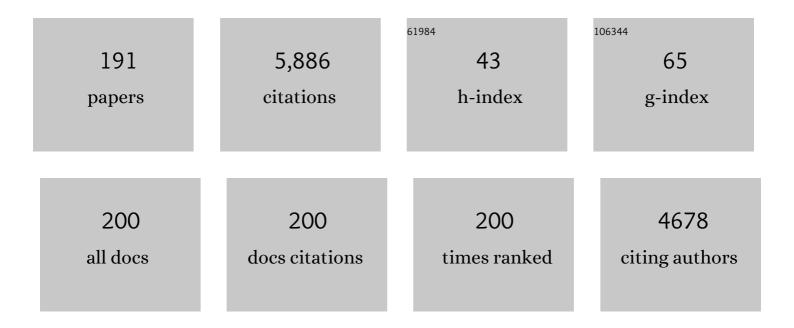
List of Publications by Year in descending order

Source: https://exaly.com/author-pdf/1588266/publications.pdf Version: 2024-02-01



#	Article	IF	CITATIONS
1	A superior fluorescent sensor for Al ³⁺ and UO ₂ ²⁺ based on a Co(<scp>ii</scp>) metal–organic framework with exposed pyrimidyl Lewis base sites. Journal of Materials Chemistry A, 2017, 5, 13079-13085.	10.3	287
2	Assembly of silver Trigons into a buckyball-like Ag ₁₈₀ nanocage. Proceedings of the National Academy of Sciences of the United States of America, 2017, 114, 12132-12137.	7.1	177
3	Anisotropic Assembly of Ag ₅₂ and Ag ₇₆ Nanoclusters. Journal of the American Chemical Society, 2018, 140, 1600-1603.	13.7	169
4	Metal–Organic Gels from Silver Nanoclusters with Aggregationâ€Induced Emission and Fluorescenceâ€toâ€Phosphorescence Switching. Angewandte Chemie - International Edition, 2020, 59, 9922-9927.	13.8	138
5	Trapping an octahedral Ag6 kernel in a seven-fold symmetric Ag56 nanowheel. Nature Communications, 2018, 9, 2094.	12.8	129
6	Different Silver Nanoparticles in One Crystal: Ag ₂₁₀ (^{<i>i</i>} PrPhS) ₇₁ (Ph ₃ P) ₅ Cl and Ag ₂₁₁ ((sup> <i>i</i> PrPhS) ₇₁ (Ph ₃ P) ₆ Cl. Angewandte Chemie - International Edition, 2019, 58, 195-199.	13.8	118
7	Deciphering synergetic core-shell transformation from [Mo6O22@Ag44] to [Mo8O28@Ag50]. Nature Communications, 2018, 9, 4407.	12.8	113
8	Beyond Clusters: Supramolecular Networks Selfâ€Assembled from Nanosized Silver Clusters and Inorganic Anions. Chemistry - A European Journal, 2016, 22, 6830-6836.	3.3	110
9	Semitransparent organic solar cells exhibiting 13.02% efficiency and 20.2% average visible transmittance. Journal of Materials Chemistry A, 2021, 9, 6797-6804.	10.3	106
10	Polymorphism in Atomically Precise Cu ₂₃ Nanocluster Incorporating Tetrahedral [Cu ₄] ⁰ Kernel. Journal of the American Chemical Society, 2020, 142, 5834-5841.	13.7	103
11	pH-Responsive Nanovesicles with Enhanced Emission Co-Assembled by Ag(I) Nanoclusters and Polyethyleneimine as a Superior Sensor for Al ³⁺ . ACS Applied Materials & Interfaces, 2018, 10, 3955-3963.	8.0	94
12	Semitransparent polymer solar cells with 9.06% efficiency and 27.1% average visible transmittance obtained by employing a smart strategy. Journal of Materials Chemistry A, 2019, 7, 7025-7032.	10.3	94
13	Amino acids-incorporated nanoflowers with an intrinsic peroxidase-like activity. Scientific Reports, 2016, 6, 22412.	3.3	93
14	Controllable all-fiber generation/conversion of circularly polarized orbital angular momentum beams using long period fiber gratings. Nanophotonics, 2018, 7, 287-293.	6.0	87
15	A hierarchically assembled 88-nuclei silver-thiacalix[4]arene nanocluster. Nature Communications, 2020, 11, 308.	12.8	86
16	Chalcogens-Induced Ag ₆ Z ₄ @Ag ₃₆ (Z = S or Se) Core–Shell Nanoclusters: Enlarged Tetrahedral Core and Homochiral Crystallization. Journal of the American Chemical Society, 2019, 141, 17884-17890.	13.7	76
17	Gold-doped silver nanocluster [Au ₃ Ag ₃₈ (SCH ₂ Ph) ₂₄ X ₅] ^{2â^'} (X) Tj £T Qq1	1 03784314
18	Anion-templated nanosized silver clusters protected by mixed thiolate and diphosphine. Nanoscale, 2017, 9, 3601-3608.	5.6	71

#	Article	IF	CITATIONS
19	Both hydrolytic and transesterification activities of Penicillium expansum lipase are significantly enhanced in ionic liquid [BMIm][PF6]. Journal of Molecular Catalysis B: Enzymatic, 2010, 63, 23-30.	1.8	66
20	A rationally-designed synergetic polypyrrole/graphene bilayer actuator. Journal of Materials Chemistry, 2012, 22, 4015.	6.7	66
21	Microporous Cd(II) metal-organic framework as fluorescent sensor for nitroaromatic explosives at the sub-ppm level. Journal of Molecular Structure, 2016, 1107, 1-6.	3.6	66
22	Microwave-assisted fatty acid methyl ester production from soybean oil by Novozym 435. Green Chemistry, 2010, 12, 844.	9.0	64
23	Carboxylic acid stimulated silver shell isomerism in a triple core–shell Ag ₈₄ nanocluster. Chemical Science, 2019, 10, 4862-4867.	7.4	63
24	Johnson Solids: Anionâ€Templated Silver Thiolate Clusters Capped by Sulfonate. Chemistry - A European Journal, 2018, 24, 1640-1650.	3.3	61
25	A Water-Stable Cl@Ag ₁₄ Cluster Based Metal–Organic Open Framework for Dichromate Trapping and Bacterial Inhibition. Inorganic Chemistry, 2017, 56, 11891-11899.	4.0	60
26	Unusual fcc-structured Ag ₁₀ kernels trapped in Ag ₇₀ nanoclusters. Chemical Science, 2019, 10, 564-568.	7.4	60
27	A Keplerian Ag90 nest of Platonic and Archimedean polyhedra in different symmetry groups. Nature Communications, 2020, 11, 3316.	12.8	60
28	Core Modulation of 70â€Nuclei Coreâ€Shell Silver Nanoclusters. Angewandte Chemie - International Edition, 2019, 58, 6276-6279.	13.8	59
29	Over 15.7% Efficiency of Ternary Organic Solar Cells by Employing Two Compatible Acceptors with Similar LUMO Levels. Small, 2020, 16, e2000441.	10.0	59
30	Terahertz imaging with sub-wavelength resolution by femtosecond laser filament in air. Scientific Reports, 2014, 4, 3880.	3.3	58
31	Impacts of daily intakes on the isomeric profiles of perfluoroalkyl substances (PFASs) in human serum. Environment International, 2016, 89-90, 62-70.	10.0	57
32	Revealing the chirality origin and homochirality crystallization of Ag14 nanocluster at the molecular level. Nature Communications, 2021, 12, 4966.	12.8	57
33	Robust Cluster Building Unit: Icosanuclear Heteropolyoxocopperate Templated by Carbonate. Chemistry - A European Journal, 2015, 21, 18847-18854.	3.3	56
34	Self-assembly of water-soluble silver nanoclusters: superstructure formation and morphological evolution. Nanoscale, 2017, 9, 19191-19200.	5.6	56
35	Recent Progress in Inorganic Anions Templated Silver Nanoclusters: Synthesis, Structures and Properties. Chemical Record, 2020, 20, 389-402.	5.8	54
36	Self-Assembly-Driven Aggregation-Induced Emission of Silver Nanoclusters for Light Conversion and Temperature Sensing. ACS Applied Nano Materials, 2020, 3, 2038-2046.	5.0	54

#	Article	IF	CITATIONS
37	A Pyridazine-Bridged Sandwiched Cluster Incorporating Planar Hexanuclear Cobalt Ring and Bivacant Phosphotungstate. Inorganic Chemistry, 2016, 55, 9006-9011.	4.0	52
38	pH-guided self-assembly of silver nanoclusters with aggregation-induced emission for rewritable fluorescent platform and white light emitting diode application. Journal of Colloid and Interface Science, 2020, 567, 235-242.	9.4	52
39	A 34â€Electron Superatom Ag ₇₈ Cluster with Regioselective Ternary Ligands Shells and Its 2D Rhombic Superlattice Assembly. Angewandte Chemie - International Edition, 2021, 60, 4231-4237.	13.8	50
40	A green and one-pot synthesis of benzo[g]chromene derivatives through a multi-component reaction catalyzed by lipase. RSC Advances, 2015, 5, 5213-5216.	3.6	49
41	A giant 90-nucleus silver cluster templated by hetero-anions. Chemical Communications, 2018, 54, 4461-4464.	4.1	49
42	Eliminationâ€Fusion Selfâ€Assembly of a Nanometer‣cale 72â€Nucleus Silver Cluster Caging a Pair of [EuW ₁₀ O ₃₆] ^{9â^²} Polyoxometalates. Chemistry - A European Journal, 2018, 24, 1998-2003.	3.3	48
43	Immobilization of Lactobacillus rhamnosus in mesoporous silica-based material: An efficiency continuous cell-recycle fermentation system for lactic acid production. Journal of Bioscience and Bioengineering, 2016, 121, 645-651.	2.2	46
44	Supramolecular Chirality from Hierarchical Self-Assembly of Atomically Precise Silver Nanoclusters Induced by Secondary Metal Coordination. ACS Nano, 2021, 15, 15910-15919.	14.6	42
45	Microwave-assisted resolution of (R,S)-2-octanol by enzymatic transesterification. Journal of Molecular Catalysis B: Enzymatic, 2007, 48, 51-57.	1.8	41
46	Rational design of a rapid fluorescent approach for detection of inorganic fluoride in MeCN–H ₂ O: a new fluorescence switch based on N-aryl-1,8-naphthalimide. New Journal of Chemistry, 2014, 38, 884-888.	2.8	41
47	Immobilization of Pseudomonas fluorescens Lipase onto Magnetic Nanoparticles for Resolution of 2-Octanol. Applied Biochemistry and Biotechnology, 2012, 168, 697-707.	2.9	39
48	Enzyme catalytic promiscuity: lipase catalyzed synthesis of substituted 2H-chromenes by a three-component reaction. RSC Advances, 2014, 4, 25633.	3.6	38
49	New protective ligands for atomically precise silver nanoclusters. Dalton Transactions, 2020, 49, 5406-5415.	3.3	38
50	Anionâ€Templated Nanosized Silver Alkynyl Clusters: Cluster Engineering and Solution Behavior. Chemistry - A European Journal, 2017, 23, 3432-3437.	3.3	36
51	An Octanuclear Cobalt Cluster Protected by Macrocyclic Ligand: In Situ Ligand-Transformation-Assisted Assembly and Single-Molecule Magnet Behavior. Inorganic Chemistry, 2020, 59, 5683-5693.	4.0	36
52	A Sodaliteâ€Type Silver Orthophosphate Cluster in a Globular Silver Nanocluster. Angewandte Chemie - International Edition, 2020, 59, 12659-12663.	13.8	36
53	Resolution of 2-octanol by SBA-15 immobilized Pseudomonas sp. lipase. Journal of Molecular Catalysis B: Enzymatic, 2007, 48, 64-69.	1.8	35
54	Near-Infrared Emitters: Stepwise Assembly of Two Heteropolynuclear Clusters with Tunable Ag ^I :Zn ^{II} Ratio. Inorganic Chemistry, 2016, 55, 4757-4763.	4.0	35

#	Article	IF	CITATIONS
55	A Dual-Protein Cascade Reaction for the Regioselective Synthesis of Quinoxalines. Organic Letters, 2020, 22, 3900-3904.	4.6	35
56	Preparation of a Flower-Like Immobilized D-Psicose 3-Epimerase with Enhanced Catalytic Performance. Catalysts, 2018, 8, 468.	3.5	34
57	Different Silver Nanoparticles in One Crystal: Ag ₂₁₀ (^{<i>i<i i=""></i></i>} PrPhS) ₇₁ (Ph ₃ P) ₅ Cl and Ag ₂₁₁ (^{<i>i<i i=""></i></i>} PrPhS) ₇₁ (Ph ₃ P) ₆ Cl. Angewandte Chemie, 2019, 131, 201-205.	2.0	34
58	Benzoateâ€Induced Highâ€Nuclearity Silver Thiolate Clusters. Chemistry - A European Journal, 2018, 24, 4967-4972.	3.3	33
59	Precise Implantation of an Archimedean Ag@Cu ₁₂ Cuboctahedron into a Platonic Cu ₄ Bis(diphenylphosphino)hexane ₆ Tetrahedron. ACS Nano, 2021, 15, 8733-8741.	14.6	33
60	Immobilization of Laccase for Oxidative Coupling of Trans-Resveratrol and Its Derivatives. International Journal of Molecular Sciences, 2012, 13, 5998-6008.	4.1	32
61	Hierarchical Nanostructures Self-Assembled by Polyoxometalate and Alkylamine for Photocatalytic Degradation of Dye. Langmuir, 2017, 33, 13242-13251.	3.5	32
62	Stepwise Assembly of Ag ₄₂ Nanocalices Based on a Mo ^{VI} -Anchored Thiacalix[4]arene Metalloligand. ACS Nano, 2022, 16, 4500-4507.	14.6	32
63	Janus Cluster: Asymmetric Coverage of a Ag ₄₃ Cluster on the Symmetric Preyssler P ₅ W ₃₀ Polyoxometalate. Chemistry of Materials, 2021, 33, 9708-9714.	6.7	32
64	Strong Spatial Confinement of Terahertz Wave inside Femtosecond Laser Filament. ACS Photonics, 2016, 3, 2338-2343.	6.6	31
65	Enantioselective transesterification of (R,S)-2-pentanol catalyzed by a new flower-like nanobioreactor. RSC Advances, 2014, 4, 33998-34002.	3.6	30
66	Enclosing classical polyoxometallates in silver nanoclusters. Nanoscale, 2019, 11, 10927-10931.	5.6	30
67	Enantioselective esterification of ibuprofen by a novel thermophilic Biocatalyst: APE1547. Biotechnology and Bioprocess Engineering, 2011, 16, 638-644.	2.6	29
68	A Green Chemoenzymatic Process for the Synthesis of Azoxybenzenes. ChemCatChem, 2015, 7, 3450-3453.	3.7	29
69	Small size yet big action: a simple sulfate anion templated a discrete 78-nuclearity silver sulfur nanocluster with a multishell structure. Chemical Communications, 2018, 54, 2361-2364.	4.1	29
70	An Ultrastable 155â€Nuclei Silver Nanocluster Protected by Thiacalix[4]arene and Cyclohexanethiol for Photothermal Conversion. Angewandte Chemie - International Edition, 2022, 61, .	13.8	29
71	Solvent-Induced Isomeric Cu ₁₃ Nanoclusters: Chlorine to Copper Charge Transfer Boosting Molecular Oxygen Activation in Sulfide Selective Oxidation. ACS Nano, 2022, 16, 9598-9607.	14.6	28
72	Thermo-Economic Performance Analysis of a Regenerative Superheating Organic Rankine Cycle for Waste Heat Recovery. Energies, 2017, 10, 1593.	3.1	27

#	Article	IF	CITATIONS
73	A novel 58-nuclei silver nanowheel encapsulating a subvalent Ag64+ kernel. Science China Chemistry, 2020, 63, 16-20.	8.2	27
74	Keplerate Ag ₁₉₂ Cluster with 6 Silver and 14 Chalcogenide Octahedral and Tetrahedral Shells. Journal of the American Chemical Society, 2021, 143, 13235-13244.	13.7	27
75	Solventâ€Controlled Condensation of [Mo ₂ O ₅ (PTC4A) ₂] ^{6â^'} Metalloligand in Stepwise Assembly of Hexagonal and Rectangular Ag ₁₈ Nanoclusters. Angewandte Chemie - International Edition. 2022. 61	13.8	27
76	Self-Assembly of Peptide-Polyoxometalate Hybrid Sub-Micrometer Spheres for Photocatalytic Degradation of Methylene Blue. Journal of Physical Chemistry B, 2017, 121, 10566-10573.	2.6	26
77	Hierarchical multi-shell 66-nuclei silver nanoclusters trapping subvalent Ag ₆ kernels. Chemical Communications, 2019, 55, 10296-10299.	4.1	26
78	In Situ Capture of a Ternary Supramolecular Cluster in a 58-Nuclei Silver Supertetrahedron. CCS Chemistry, 2022, 4, 1788-1795.	7.8	26
79	Using Laccases in the Nanoflower to Synthesize Viniferin. Catalysts, 2017, 7, 188.	3.5	25
80	Investigation of the pro-apoptotic effects of arbutin and its acetylated derivative on murine melanoma cells. International Journal of Molecular Medicine, 2018, 41, 1048-1054.	4.0	25
81	Application of dual-enzyme nanoflower in the epoxidation of alkenes. Process Biochemistry, 2018, 74, 103-107.	3.7	25
82	A chemo-enzymatic process for sequential kinetic resolution of (R,S)-2-octanol under microwave irradiation. Process Biochemistry, 2007, 42, 1312-1318.	3.7	24
83	A lipase–glucose oxidase system for the efficient oxidation of N-heteroaromatic compounds and tertiary amines. Green Chemistry, 2016, 18, 3518-3521.	9.0	24
84	Lipase-Catalyzed Synthesis of Indolyl 4H-Chromenes via a Multicomponent Reaction in Ionic Liquid. Catalysts, 2017, 7, 185.	3.5	24
85	Amphiphilicity Regulation of Ag ^I Nanoclusters: Selfâ€Assembly and Its Application as a Luminescent Probe. Chemistry - A European Journal, 2019, 25, 4713-4721.	3.3	24
86	Lipase catalyzed synthesis of 3,3′-(arylmethylene)bis(2-hydroxynaphthalene-1,4-dione). RSC Advances, 2014, 4, 35686-35689.	3.6	23
87	pH-Controlled assembly of two novel Dawson-sandwiched clusters involving the in situ reorganization of trivacant α-[P ₂ W ₁₅ O ₅₆] ^{12â^'} into divacant α-[P ₂ HO ₅₇] ^{8â^'} . Dalton Transactions, 2016, 45. 8404-8411.	3.3	23
88	Anionic passivation layer-assisted trapping of an icosahedral Ag13 kernel in a truncated tetrahedral Ag89 nanocluster. Science China Chemistry, 2021, 64, 1482-1486.	8.2	23
89	Cloning, Expression and Characterization of a Novel Thermophilic Polygalacturonase from Caldicellulosiruptor bescii DSM 6725. International Journal of Molecular Sciences, 2014, 15, 5717-5729.	4.1	22
90	Lipase-catalyzed Knoevenagel condensation between α,β-unsaturated aldehydes and active methylene compounds. Chinese Chemical Letters, 2014, 25, 802-804.	9.0	22

#	Article	IF	CITATIONS
91	Octanuclear Ni(<scp>ii</scp>) cubes based on halogen-substituted pyrazolates: synthesis, structure, electrochemistry and magnetism. CrystEngComm, 2016, 18, 3462-3471.	2.6	22
92	Structure advantage and peroxidase activity enhancement of deuterohemin-peptide–inorganic hybrid flowers. RSC Advances, 2016, 6, 104265-104272.	3.6	22
93	Silver clusters templated by homo- and hetero-anions. CrystEngComm, 2020, 22, 3736-3748.	2.6	22
94	Supramolecular Self-Assembly of Atomically Precise Silver Nanoclusters with Chiral Peptide for Temperature Sensing and Detection of Arginine. Nanomaterials, 2022, 12, 424.	4.1	21
95	The effect of ultrasound on lipase-catalyzed regioselective acylation of mangiferin in non-aqueous solvents. Journal of Asian Natural Products Research, 2010, 12, 56-63.	1.4	20
96	Microwave-assisted enzymatic resolution of (R,S)-2-octanol in ionic liquid. Process Biochemistry, 2012, 47, 479-484.	3.7	19
97	Silver–Sulfur Hybrid Supertetrahedral Clusters: The Hitherto Missing Members in the Metal–Chalcogenide Tetrahedral Clusters. Chemistry - A European Journal, 2017, 23, 14420-14424.	3.3	19
98	An Improved Method to Encapsulate Laccase from Trametes versicolor with Enhanced Stability and Catalytic Activity. Catalysts, 2018, 8, 286.	3.5	19
99	Core Modulation of 70â€Nuclei Coreâ€Shell Silver Nanoclusters. Angewandte Chemie, 2019, 131, 6342-6345.	2.0	19
100	Nuclearity enlargement from [PW9O34@Ag51] to [(PW9O34)2@Ag72] and 2D and 3D network formation driven by bipyridines. Nature Communications, 2022, 13, 1802.	12.8	19
101	Regioselective acylation of resveratrol catalyzed by lipase under microwave. Green Chemistry Letters and Reviews, 2018, 11, 312-317.	4.7	18
102	Optimization of APE1547-catalyzed enantioselective transesterification of (R/S)-2-methyl-1-butanol in an ionic liquid. Biotechnology and Bioprocess Engineering, 2011, 16, 337-342.	2.6	17
103	Three Silver Nests Capped by Thiolate/Phenylphosphonate. Chemistry - A European Journal, 2018, 24, 15096-15103.	3.3	17
104	Facile Fabrication of a Novel Copper Nanozyme for Efficient Dye Degradation. ACS Omega, 2021, 6, 6284-6291.	3.5	17
105	Circularly Polarized Phosphorescence from Cocrystallization of Atomic Precise Silver Nanoclusters with Tartaric Acid. Advanced Optical Materials, 2022, 10, .	7.3	17
106	Synthesis of 2-Ethylhexyl Palmitate Catalyzed by Enzyme Under Microwave. Applied Biochemistry and Biotechnology, 2018, 185, 347-356.	2.9	16
107	Realizing enhanced luminescence of silver nanocluster–peptide soft hydrogels by PEI reinforcement. Soft Matter, 2018, 14, 8352-8360.	2.7	16
108	A Sodaliteâ€Type Silver Orthophosphate Cluster in a Globular Silver Nanocluster. Angewandte Chemie, 2020, 132, 12759-12763.	2.0	16

#	Article	IF	CITATIONS
109	Magnetocaloric effect in multiferroic Y-type hexaferrite Ba0.5Sr1.5Zn2(Fe0.92Al0.08)12O22. AIP Advances, 2014, 4, .	1.3	15
110	An efficient condensation of substituted salicylaldehyde and malononitrile catalyzed by lipase under microwave irradiation. RSC Advances, 2015, 5, 57122-57126.	3.6	15
111	Kagóme Cobalt(II)â€Organic Layers as Robust Scaffolds for Highly Efficient Photocatalytic Oxygen Evolution. ChemSusChem, 2016, 9, 1146-1152.	6.8	15
112	Synthesis of dihydropyrano[4,3- <i>b</i>]pyranes via a multi-component reaction catalyzed by lipase. Green Chemistry Letters and Reviews, 2017, 10, 54-58.	4.7	15
113	A Polyoxochromate Templated 56-Nuclei Silver Nanocluster. Inorganic Chemistry, 2020, 59, 3004-3011.	4.0	15
114	Improvement of the enantioselectivity and activity of lipase from <i>Pseudomonas</i> sp. via adsorption on a hydrophobic support: kinetic resolution of 2-octanol. Biocatalysis and Biotransformation, 2009, 27, 340-347.	2.0	14
115	Construction of hydroxypropyl-β-cyclodextrin copolymer nanoparticles and targeting delivery of paclitaxel. Journal of Nanoparticle Research, 2012, 14, 1.	1.9	14
116	Improving the properties of β-galactosidase from Aspergillus oryzae via encapsulation in aggregated silica nanoparticles. New Journal of Chemistry, 2013, 37, 3793.	2.8	14
117	Multifaceted Bicubane Co4Clusters: Magnetism, Photocatalytic Oxygen Evolution, and Electrical Conductivity. European Journal of Inorganic Chemistry, 2016, 2016, 3253-3261.	2.0	14
118	Double telecom band thermo-optic switch based on dual-line filled photonic liquid crystal fibres. Liquid Crystals, 2017, 44, 479-483.	2.2	14
119	A mild and efficient Dakin reaction mediated by lipase. Green Chemistry Letters and Reviews, 2017, 10, 269-273.	4.7	14
120	Tatarinan N inhibits osteoclast differentiation through attenuating NF-κB, MAPKs and Ca2+-dependent signaling. International Immunopharmacology, 2018, 65, 199-211.	3.8	14
121	Metal–Organic Gels from Silver Nanoclusters with Aggregationâ€Induced Emission and Fluorescenceâ€toâ€Phosphorescence Switching. Angewandte Chemie, 2020, 132, 10008-10013.	2.0	14
122	Observation of a bcc-like framework in polyhydrido copper nanoclusters. Nanoscale, 2021, 13, 19642-19649.	5.6	14
123	Enantioselective transesterification of glycidol catalysed by a novel lipase expressed fromBacillus subtilis. Biotechnology and Applied Biochemistry, 2010, 56, 1-6.	3.1	13
124	Resolution of <i>N</i> â€hydroxymethyl vince lactam catalyzed by lipase in organic solvent. Journal of Chemical Technology and Biotechnology, 2013, 88, 904-909.	3.2	13
125	Coupled Model of Heat and Mass Balance for Droplet Growth in Wet Steam Non-Equilibrium Homogeneous Condensation Flow. Energies, 2017, 10, 2033.	3.1	13
126	Enantioselective enzymatic hydrolysis of racemic glycidyl butyrate by lipase from Bacillus subtilis with improved catalytic properties. Journal of Molecular Catalysis B: Enzymatic, 2008, 55, 152-156.	1.8	12

#	Article	IF	CITATIONS
127	Chemoenzymatic Synthesis of αâ€Â€yano Epoxides by a Tandemâ€ÂKnoevenagel–Epoxidation Reaction. European Journal of Organic Chemistry, 2016, 2016, 1251-1254.	2.4	12
128	Lipase-Mediated Amidation of Anilines with 1,3-Diketones via C–C Bond Cleavage. Catalysts, 2017, 7, 115.	3.5	12
129	Fabrication of a nano-biocatalyst for regioselective acylation of arbutin. Green Chemistry Letters and Reviews, 2018, 11, 55-61.	4.7	12
130	Fabrication of a novel nano-biosensor for efficient colorimetric determination of uric acid. Applied Nanoscience (Switzerland), 2022, 12, 2255-2264.	3.1	12
131	Highly efficient and regioselective acylation of arbutin catalyzed by lipase from Candida sp Process Biochemistry, 2015, 50, 789-792.	3.7	11
132	Ultrasound-Assisted Enantioselective Esterification of Ibuprofen Catalyzed by a Flower-Like Nanobioreactor. Molecules, 2016, 21, 565.	3.8	11
133	Synthesis of functionalized 4H-Chromenes catalyzed by lipase immobilized on magnetic nanoparticles. Green Chemistry Letters and Reviews, 2018, 11, 246-253.	4.7	11
134	An Extended Ag ^I Clusterâ€Based Framework Solid: Silverâ€Thiolate Cluster Linked Polyoxometalate Including Ag ^I ···H–C Anagostic Interactions. European Journal of Inorganic Chemistry, 2019, 2019, 496-501.	2.0	11
135	A two-step enzymatic resolution of glycidyl butyrate. Process Biochemistry, 2007, 42, 1319-1325.	3.7	10
136	Combining the Physical Adsorption Approach and the Covalent Attachment Method to Prepare a Bifunctional Bioreactor. International Journal of Molecular Sciences, 2012, 13, 11443-11454.	4.1	10
137	Numeric simulation of wet-steam two-phase condensing flow in a steam turbine cascade. Journal of the Brazilian Society of Mechanical Sciences and Engineering, 2017, 39, 1189-1199.	1.6	10
138	A 34â€Electron Superatom Ag 78 Cluster with Regioselective Ternary Ligands Shells and Its 2D Rhombic Superlattice Assembly. Angewandte Chemie, 2021, 133, 4277-4283.	2.0	10
139	Luminescent Hydrogel Based on Silver Nanocluster/Malic Acid and Its Composite Film for Highly Sensitive Detection of Fe3+. Gels, 2021, 7, 192.	4.5	10
140	Enantioselective Esterification of Ibuprofen under Microwave Irradiation. Molecules, 2013, 18, 5472-5481.	3.8	9
141	A Novel Oxidation of Salicyl Alcohols Catalyzed by Lipase. Catalysts, 2017, 7, 354.	3.5	9
142	The design and characterization of a hypersensitive glucose sensor: two enzymes co-fixed on a copper phosphate skeleton. Journal of Materials Chemistry B, 2020, 8, 244-250.	5.8	9
143	Ultrasound Irradiation Promoted Enzymatic Transesterification of (R/S)-1-Chloro-3-(1-naphthyloxy)-2-propanol. Molecules, 2012, 17, 10864-10874.	3.8	8
144	A new method for the enamination of 1,3-dicarbonyl compounds catalyzed by laccase in water. RSC Advances, 2014, 4, 19512-19515.	3.6	8

#	Article	IF	CITATIONS
145	Kinetic resolution of (<i>R, S</i>)â€2â€{2â€chloroâ€1â€hydroxyethyl) thiophene via immobilizing lipase from <i>Alcaligenes sp</i> . onto magnetic nanoparticles. Journal of Chemical Technology and Biotechnology, 2015, 90, 492-499.	3.2	8
146	Selfâ€Assembly of A Novel Ag 48 Cluster Encapsulating an Unprecedented [Mo 8 O 28] 8â^' Anion Template. Israel Journal of Chemistry, 2019, 59, 280-285.	2.3	8
147	Microwave-Assisted Resolution of Î \pm -Lipoic Acid Catalyzed by an Ionic Liquid Co-Lyophilized Lipase. Molecules, 2015, 20, 9949-9960.	3.8	7
148	Enantioselective transesterification ofN-hydroxymethyl vince lactam catalyzed by lipase under ultrasound irradiation. Biocatalysis and Biotransformation, 2013, 31, 299-304.	2.0	6
149	Magnetic and Dielectric Properties in Multiferroic Y-type Hexaferrite. Molecular Crystals and Liquid Crystals, 2014, 603, 235-239.	0.9	6
150	FFT Algorithm-Assisted Polarimetric Twist Sensor. IEEE Photonics Technology Letters, 2017, 29, 2083-2086.	2.5	6
151	Tatarinan T, an αâ€asaroneâ€derived lignin, attenuates osteoclastogenesis induced by RANKL via the inhibition of NFATc1/câ€Fos expression. Cell Biology International, 2019, 43, 1471-1482.	3.0	6
152	Silica–Organometallic One-Dimensional Hybrid Employing a Agâ~'Ï€ _{Câ•C} Bond Connecting Alternating Ag ₄ (NO ₃) ₄ and Octavinylsilsesquioxane. Inorganic Chemistry, 2021, 60, 2899-2904.	4.0	6
153	Molecular Dynamic Simulations of Bromodomain and Extra-Terminal Protein 4 Bonded to Potent Inhibitors. Molecules, 2022, 27, 118.	3.8	6
154	Single Longitudinal Mode Optofluidic Microring Laser Based on a Hollow-Core Microstructured Optical Fiber. IEEE Photonics Journal, 2017, 9, 1-10.	2.0	5
155	An Improved Analysis Method for Organic Rankine Cycles Based on Radial-Inflow Turbine Efficiency Prediction. Applied Sciences (Switzerland), 2019, 9, 49.	2.5	5
156	Activity adaptability of a DhHP-6 peroxidase-mimic in wide pH and temperature ranges and solvent media. Catalysis Science and Technology, 2020, 10, 1848-1857.	4.1	5
157	Carbonate–Water Supramolecule Trapped in Silver Nanoclusters Encapsulating Unprecedented Ag ₁₁ Kernel. CCS Chemistry, 2020, 2, 663-672.	7.8	5
158	Structural rearrangement of Ag60 nanocluster endowing different luminescence performances. Journal of Chemical Physics, 2021, 155, 234303.	3.0	5
159	Addition of Diethylzinc to Aromatic Aldehydes Catalyzed by Hydrolase. Chinese Journal of Catalysis, 2009, 30, 396-400.	14.0	4
160	Switchable-multi-wavelength fiber laser based on dual-core all-solid photonic bandgap fiber. Frontiers of Optoelectronics in China, 2010, 3, 283-288.	0.2	4
161	Polyanion modulated evolution of perovskite BiFeO3 microspheres to microcubes by a microwave assisted hydrothermal method. Journal of Materials Research, 2013, 28, 1498-1504.	2.6	4
162	Enzymatic resolution of ibuprofen in an organic solvent under ultrasound irradiation. Biotechnology and Applied Biochemistry, 2014, 61, 655-659.	3.1	4

#	Article	IF	CITATIONS
163	A novel re-tracking strategy for monocular SLAM. , 2017, , .		4
164	Experimental Evaluation of Modern TCP Variants in MEC-enabled Cellular Networks. , 2018, , .		4
165	Efficient Degradation of Gas-Phase Toluene by Ozone-Assisted Photocatalytic Oxidation on TiO2/Graphene Composites. Catalysis Letters, 2019, 149, 2739-2748.	2.6	4
166	Design and Characterization of a Novel Artificial Peroxidase. Catalysts, 2019, 9, 168.	3.5	4
167	Focusing characteristics of optical vortex passing through a Fresnel zone plate. Optical Engineering, 2021, 60, .	1.0	4
168	Increases in Genetic Diversity of Weedy Rice Associated with Ambient Temperatures and Limited Gene Flow. Biology, 2021, 10, 71.	2.8	4
169	An Ultrastable 155â€Nuclei Silver Nanocluster Protected by Thiacalix[4]arene and Cyclohexanethiol for Photothermal Conversion. Angewandte Chemie, 2022, 134, .	2.0	4
170	Effects of mechanochemical activation on the structural and electrical properties of orthorhombic LuFeO 3 ceramics. Journal of the American Ceramic Society, 2021, 104, 3019-3029.	3.8	3
171	Synthesis, structures and luminescence of silver (I) thiolate nanoclusters based on anion templates. Scientia Sinica Chimica, 2017, 47, 695-704.	0.4	3
172	Solventâ€Controlled Condensation of [Mo ₂ O ₅ (PTC4A) ₂] ^{6â^'} Metalloligand in Stepwise Assembly of Hexagonal and Rectangular Ag ₁₈ Nanoclusters. Angewandte Chemie, 2022, 134,	2.0	3
173	Application of ring-opening metathesis polymerization in study of polymer molecular weight-mediated catalytic properties of immobilized lipase. Science Bulletin, 2009, 54, 382-386.	9.0	2
174	Deep notch filter based on liquid-filled photonic crystal fiber. Frontiers of Optoelectronics in China, 2010, 3, 289-291.	0.2	2
175	Resolution of 1,1,1-trifluoro-2-octanol by Pseudomonas sp. lipase encapsulated in aggregated silica nanoparticles. RSC Advances, 2014, 4, 6103.	3.6	2
176	Ultrasound promoted enantioselective transesterification of 3-hydroxy-3-(2-thienyl) propanenitrile catalyzed by lipase. Green Chemistry Letters and Reviews, 2016, 9, 190-195.	4.7	2
177	Effect of Candesartan cilexetil as a sensitive and effective inhibitor of SHP-1 on insulin signaling pathway. Chemical Research in Chinese Universities, 2013, 29, 730-734.	2.6	1
178	[Ag ₂₅ (SC ₆ H ₄ Pr <i>ⁱ</i>) ₁₈ (dppp) _{6(HSC₆H₄Pr<i>ⁱ</i> = 4-<i>t</i>/i>-isopropylthiophenol, and dppp = 1,) Tj E Characterization and Optical Properties. Wuli Huaxue Xuebao/ Acta Physico - Chimica Sinica, 2018, 34,}	b>](CF <si TQq0 0 0 4.9</si 	ub>3SC rgBT /Overlock 1
179	776-780. Distributed hybrid-fiber Raman amplifiers with a section of nonlinear microstructured optical fiber. Microwave and Optical Technology Letters, 2006, 48, 2267-2271.	1.4	0
180	All-Optical Clock Frequency Multiplication Based on SOA-assisted Mach-Zehnder Interfering. , 2008, , .		0

#	Article	IF	CITATIONS
181	Pose determination from airborne LiDAR data and onboard image for future driver assistance systems. , 2011, , .		0
182	Synthesis of Triptorelin Lactate Catalyzed by Lipase in Organic Media. International Journal of Molecular Sciences, 2012, 13, 9971-9979.	4.1	0
183	A high sensitivity temperature sensor based on a selectively filled photonic crystal fiber sagnac interferometer. , 2012, , .		0
184	Parameter designing to improve the energy efficiency of quantum dot semiconductor optical amplifier. Microwave and Optical Technology Letters, 2015, 57, 896-901.	1.4	0
185	All-optical repetition rate multiplication of pseudorandom bit sequences by employing power coupler and equalizer. Optical Engineering, 2015, 54, 106111.	1.0	0
186	Solving the Hamiltonian path problem using optical fiber network. , 2016, , .		0
187	Fiber interferometric probe based on a long period grating inscribed in an all-solid photonic bandgap fiber. , 2016, , .		0
188	Coupling Characteristics of Selective-Infiltration-Based Locally Tapered Photonic Crystal Fiber. IEEE Photonics Journal, 2017, 9, 1-7.	2.0	0
189	Single mode excitation ring resonator dye laser based on simplified hollow-core microstructured optical fiber. , 2017, , .		0
190	Innentitelbild: Core Modulation of 70â€Nuclei Coreâ€Shell Silver Nanoclusters (Angew. Chem. 19/2019). Angewandte Chemie, 2019, 131, 6168-6168.	2.0	0
191	Innentitelbild: A Sodaliteâ€Type Silver Orthophosphate Cluster in a Globular Silver Nanocluster (Angew. Chem. 31/2020). Angewandte Chemie, 2020, 132, 12646-12646.	2.0	Ο